

## REINFORCEMENT LOADS IN GEOSYNTHETIC WALLS AND THE CASE FOR A NEW WORKING STRESS DESIGN METHOD

Richard J. Bathurst, GeoEngineering Centre at Queen's-RMC, Royal Military College, Kingston, Ontario  
Tony Allen, Washington State Department of Transportation, Olympia, Washington, USA  
Dave Walters, GeoEngineering Centre at Queen's-RMC, Queen's University, Kingston, Ontario

**abstract:** The paper provides a synthesis of work by the writers that has the objective of developing a new working stress method for the calculation of reinforcement loads in geosynthetic reinforced soil walls. As a precursor to this objective, careful back-analyses of a database of instrumented and monitored full-scale field and laboratory walls are used to demonstrate that the current Simplified Method used in North America results in excessively conservative estimates of the volume of reinforcement required to generate satisfactory long-term wall performance. The new design method captures the essential contributions of the different wall components and properties to reinforcement loads. The method is calibrated against measured in-situ wall reinforcement loads using a careful interpretation of reinforcement strains and the conversion of strain to load using a suitably selected reinforcement stiffness value. A novel feature of the method is to design the wall reinforcement so that the soil within the wall backfill is prevented from reaching a failure limit state, consistent with the notion of working stress conditions.

**RÉSUMÉ:** L'article fournit une synthèse du travail faite par les auteurs qui a l'objectif de développer une nouvelle méthode de contraintes admissibles pour le calcul des charges de renforcement dans des murs de sol renforcés par les géosynthétiques. Comme précurseur à cet objectif, des analyses soigneuses d'une base de données des murs équipés de laboratoire et in-situ sont employées pour démontrer que la méthode simplifiée courante employée en Amérique du Nord a comme conséquence des évaluations excessivement conservatrices du volume du renforcement, exigé pour assurer une performance satisfaisante de mur à long terme. La nouvelle méthode de conception capture les contributions essentielles des différents composants et propriétés de mur aux charges de renforcement. La méthode est calibrée contre les charges de renforcement, mesurées in-situ, en utilisant une interprétation soignée des déformations de renforcement et de la conversion de la déformation en charge en utilisant une valeur convenablement choisie de la rigidité de renforcement. Une nouvelle caractéristique de la méthode est de concevoir le renforcement de sorte que le sol dans le mur soit empêché d'atteindre l'état limite de la rupture, conformément à la notion des contraintes admissibles.

### 1. INTRODUCTION

Geosynthetic-reinforced soil walls have been in use for more than 25 years and in the vast majority of cases have performed very well. Nevertheless, the inherent margin of safety against poor performance with respect to internal stability has not been quantified in a systematic manner. This lack of quantification can be argued to contribute to the current lack of acceptance for this technology by some practitioners and government agencies in North America.

The paper reviews evidence of the conservatism in current North American practice for geosynthetic-reinforced soil walls with respect to design for internal stability. The quantitative assessment of conservatism is based on data collected from carefully selected instrumented and monitored geosynthetic-reinforced field structures in North America, Europe and Scandinavia, and full-scale laboratory walls constructed at the Royal Military College of Canada (RMC). An additional acceptance criterion for the case studies was the availability of project-specific or closely related laboratory test data for the component reinforcement materials and reliable strength data for the granular soil backfill. The data taken from case studies have been used to identify sources of conservatism in current North American practice and identify quantitative behaviour with regard to

magnitude and distribution of reinforcement loads at the end of construction and beyond.

A fundamental requirement to assess conservatism in current design practice and to validate new design approaches is a reliable estimate of the load in reinforcement layers. However, direct measurement of reinforcement loads is rare in the case study literature. The paper describes how reinforcement strain measurements and the conversion of strain to load through the use of a properly selected reinforcement stiffness value can be used to estimate reinforcement loads. This approach also requires quantification of the reliability and accuracy of strain measurements from different instrumentation techniques.

Next the paper examines strategies to select appropriate stiffness values for geosynthetic reinforcement products based largely on interpretation of in-isolation laboratory testing, but recognising the influence of soil confinement, strain level, duration of loading and temperature amongst other factors.

Based on best estimates of reinforcement loads from the database of case studies, an empirical-based reinforcement load distribution that is trapezoidal in shape is shown to be more accurate than the triangular distribution that is assumed in current North America practice.

Finally, the paper reviews a new empirical-based design method that is demonstrated to give better predictions of internal reinforcement loads under working stress conditions when compared to values taken from the database of monitored walls.

## 2. CASE STUDIES

The writers have collected a total of 20 case histories (including 35 different wall sections) from papers published in the open literature and in some cases from unpublished sources (Allen et al. 2002). The soil reinforcement products in these structures included geotextiles and geogrids manufactured from a variety of polymers including polypropylene (PP), high density polyethylene (HDPE), and polyester (PET). The materials were strip and continuous reinforcements with a wide range of index tensile strengths from 12 to 200 kN/m, and reinforcement index stiffness values at the end of wall construction from 43 to 7,400 kN/m at 2% strain. Reinforcement vertical spacing varied from 0.3 to 1.6 m.

Wall facing batter angles varied from 0° (vertical) to 27°, although most of the walls had facing batter angles of 8° or less. Wall heights varied from 3.0 to 12.6 m, with surcharge heights of up to 5.3 m of soil. Facing types included geosynthetic wrapped-face, welded wire, pre-cast concrete panels, and modular concrete blocks.

Measured peak friction angles from triaxial or direct shear tests ranged from 39° to 49° (42° to 57° plane strain). Peak friction angles reported in the source references from triaxial compression tests on granular soils were corrected to peak plane strain friction angles using the equation by Lade and Lee (1976). Direct shear test peak friction angle values for dense sands were converted to peak plane strain values using an expression presented by Bolton (1986) and Jewell and Wroth (1987).

Most conditions that are likely to be encountered in practice are included in these case histories. All of the case histories used relatively clean granular backfills (i.e., less than 15% silt content and little, if any, plasticity), and were placed on relatively competent foundation soils. Therefore, the scope of this paper is limited to geosynthetic walls with relatively clean non-cohesive sand or gravel backfill. Finally, the wall case histories represented in this paper do not include tiered structures or walls used as bridge abutments.

## 3. EVIDENCE OF EXCESSIVE CONSERVATISM IN CURRENT PRACTICE

An approach to quantify the global margin of safety for existing geosynthetic retaining walls is to calculate the sum of reinforcement load capacities (R - resistance) and divide this value by the total horizontal earth load that is assumed to be carried by the reinforcement layers (D - demand) (Allen et al. 2002). The resistance-demand ratio (RD) can be expressed as:

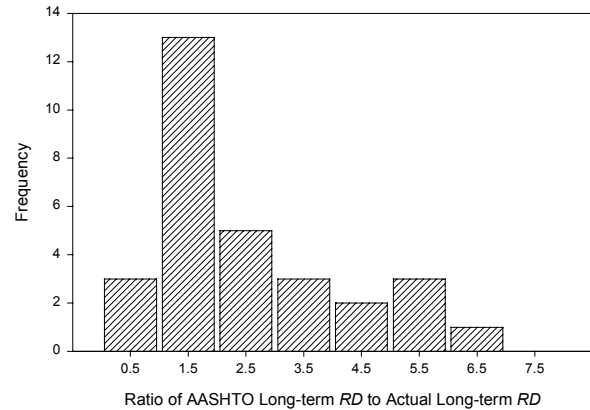


Figure 1. Degree of conservatism in long-term resistance to demand ratio when using current practice (AASHTO 2002) for case histories with good long-term performance (Allen et al. 2002).

$$RD = \frac{R}{D} = \frac{\sum_{i=1}^n T_i}{0.5 K_{ah} \gamma H^2 + K_{ah} q H} \quad [1]$$

where:  $T_i$  = reinforcement load;  $K_{ah}$  =  $K_a(\phi_{ps}, \delta, \omega) \times \cos(\delta - \omega)$  = horizontal component of active earth pressure;  $\phi_{ps}$  = the measured peak plane strain friction angle of the soil;  $\omega$  = wall batter;  $\delta$  = interface shear angle between wall facing and backfill soil (assumed to be zero based on current practice as defined by AASHTO (2002));  $H$  = total wall height measured from the toe of the wall to the soil surface immediately behind the wall facing;  $\gamma$  = the bulk unit weight of the soil and;  $q$  is the magnitude of any uniformly distributed surcharge load at the soil surface. This calculation can be carried out for conditions representing end of construction and at design-life (75 years).

Figure 1 shows the distribution of the ratio of RD values calculated using current AASHTO (2002) guidelines and RD values using best estimates of the long-term capacity of the reinforcement layers (resistance) and demand. These data are for walls that have exhibited good performance defined by (Allen and Bathurst 2002) as:

1. Reinforcement strains are small (typically less than 3%).
2. Creep strains and strain rates decrease as time increases (i.e., only primary creep observed).
3. The wall backfill soil does not exhibit signs of failure (cracking, slumping, etc.).
4. Post-construction deformations, which are typically greatest at the wall top, are less than 30 mm within the first 10,000 hours.

The data show that most existing walls would be over-designed with respect to their observed long-term good performance if the current AASHTO method is used. Put

another way, these structures appear to be significantly under-designed based on current practice. Nevertheless, careful analyses showed that walls that exhibited good performance contained less than one half the reinforcement typically required using current AASHTO specifications. In some cases only one-eighth the reinforcement was actually required. The potential to reduce excessive conservatism in current practice for the design of reinforcement is clear.

#### 4. ESTIMATION OF LOADS IN GEOSYNTHETIC REINFORCEMENT LAYERS

While the previous section has identified excessive conservatism in current design methods using a global approach to reinforcement tensile capacity and demand, convincing arguments to abandon or modify the current Simplified Method must be based on a comparison of measured loads to predicted loads. Unfortunately, direct measurement of reinforcement loads has only been reported in one case history in the literature (Fannin 1988). Typically, loads in reinforcement layers are inferred from measurements made by strain gauges or pairs of extensometers attached to the layers. This section gives a review of issues related to the interpretation of strains using different instrumentation techniques and the accuracy that may be expected from the readings. Next, techniques to properly select a reinforcement stiffness value to convert strains to load are discussed and a protocol to carryout this selection using in-isolation laboratory testing summarised.

##### 4.1 Strain Measurements

Interpretation of strain readings from devices attached to geosynthetic reinforcement layers depends on the type of device (Perkins and Lapeyre 1997). The most common types of devices are strain gauges bonded directly to the surface of the geosynthetic reinforcement material and extensometers. Displacements recorded by pairs of extensometers are used to calculate global strains assumed to be constant over the distance between monitoring points. In one case study used by the writers, inductance coils were used to infer strains.

##### 4.1.1 Strain Gauges

Small, high elongation strain gauges glued to the reinforcement material must be calibrated against the "true" global strain in the reinforcement. Strain gauges bonded to woven geogrids or geotextiles typically generate a local "hard spot" causing under-registration of global tensile strains. Strain gauges bonded to integral drawn PP and HDPE geogrids will record the local strain at the attachment point which may vary from point to point due to product geometry (cross-sectional area) and polymer modulus (result of drawing process during manufacture). The calibration factor (CF) for a particular combination of gauge, bonding technique, reinforcement type and location of gauge is typically established from constant-rate-of-strain in-isolation wide width strip tensile testing (e.g., ASTM D 4595).

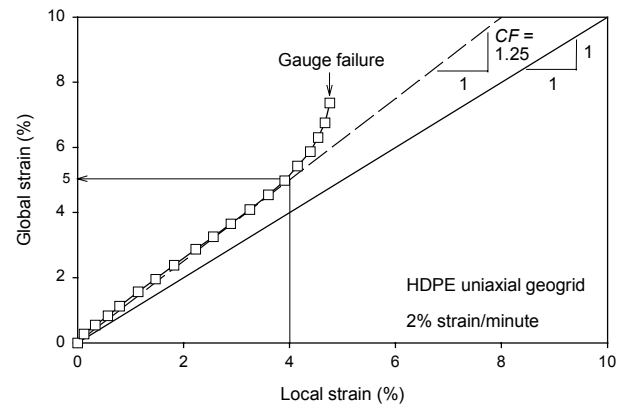


Figure 2. Example in-isolation global strain versus strain gauge response for HDPE geogrid (after Bathurst 1992).

Note: CF = calibration factor for local strain  $\leq 4\%$ .

Figure 2 demonstrates the relationship (under-registration) between global strain corresponding to the average strain over multiple apertures of a typical drawn HDPE geogrid and local strain. In this case the local strain was recorded by a single strain gauge mounted on a longitudinal member at the midpoint between adjacent transverse members.

Based on a review of available in-isolation tension test gauge calibration data the following observations have been made by Bathurst et al. (2002):

1. The magnitude of strain gauge under-registration (and hence magnitude of calibration factor CF) at a local strain of 2% is greatest for woven or knitted geotextiles and close to unity for extruded drawn PP geogrids.
2. Variability in strain gauge response is greatest for woven geotextiles.
3. Non-linearity in CF values with magnitude of global strain is greatest for woven geotextiles and geogrids and least for uniaxial HDPE geogrids. An example of non-linearity in strain response at large strains is illustrated in Figure 2.
4. In all the wall case histories reviewed, the magnitude of calibration factor was greater than or equal to unity.

For the case of extruded drawn PP geogrid specimens investigated by the writers, the interpretation of global strain was complicated by the observation that lower CF values were obtained from constant-load calibration tests compared to the results for the same materials tested under constant-rate-of-strain conditions.

##### 4.1.2 In-situ Global Strains from Extensometer Readings

A correction factor is not needed if extensometers attached to the geosynthetic are used. Nevertheless, strains inferred from extensometers may over-estimate geosynthetic yarn or rib strains as initial surface wrinkles or warps in the geosynthetic are taken up during fill

placement or under-estimate strains due to initial slackness in the extensometer cables.

#### 4.1.3 Other Devices

Inductance coil pairs attached to and in the same plane as the geogrid reinforcement have been used to infer strains. Average global strains based on sets of three devices located at the same nominal distance from the wall face were as great as 0.9% at the end of surcharging (Fannin and Hermann 1990) and were reported to have a resolution of  $\pm 0.1\%$  (Fannin 1988). These devices are calibrated in-isolation and do not require a correction factor. However, the signal from inductance coil pairs is sensitive to the magnitude of out-of-plane movements that may be generated due to fill placement, soil displacements and flexure of the reinforcement.

#### 4.1.4 Redundancy of Reinforcement Measurements

In several case studies, multiple strain gauges were placed at nominal identical locations from the wall facing. This approach allows readings to be averaged across the width of the wall and also provides redundancy in the event of failure of an individual gauge in a set of two or more gauges.

Figure 3 shows that the uncorrected response of a pair of strain gauges mounted on a PP geogrid may vary by about  $\pm 15\%$  of the mean reading of 2% strain at a prediction level of 95%.

The review of physical data from well-instrumented wall structures has allowed the writers to comment on the reliability of the strain data, both qualitatively and quantitatively (Bathurst et al. 2002). Specifically:

1. Based on data available for an instrumented drawn PP geogrid, the coefficient of variation (COV) for strain gauge readings was calculated to be 13% for strains  $\geq 0.02\%$ . Similar data for a knitted polyester geogrid gave a COV = 14% for strains  $\geq 0.1\%$ .
2. Based on data for instrumented PP geogrids, strain gauges have proved accurate to estimate reinforcement strains at low strain levels (0.02 to 2%). Extensometers are more reliable for reinforcement strains  $\geq 2\%$ . For a knitted polyester geogrid, strain gauges gave reliable readings for strains greater than 0.1%.
3. Analysis of inductance coil readings showed that these instruments gave the least reliable readings of the three measurement techniques investigated (e.g., COV = 32% for strains in the range of 0.2 to 0.9%).
4. Bonded strain gauges in the field typically gave a non-linear response or failed at strains greater than 3%, hence extensometers provide the only practical

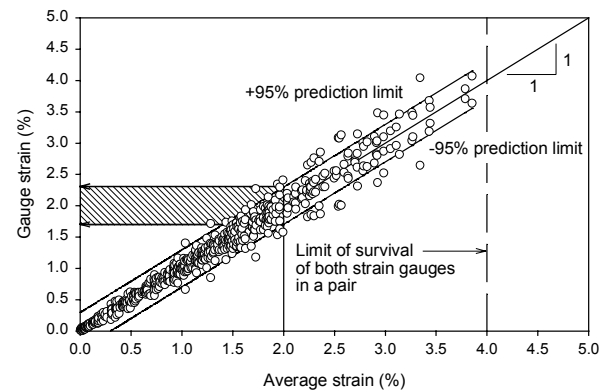


Figure 3. Variation in strain gauge response versus average of strain gauge pair mounted at nominal identical distance behind the wall face on layers of PP geogrid (Bathurst et al. 2002).

means of estimating reinforcement strains at large strain levels.

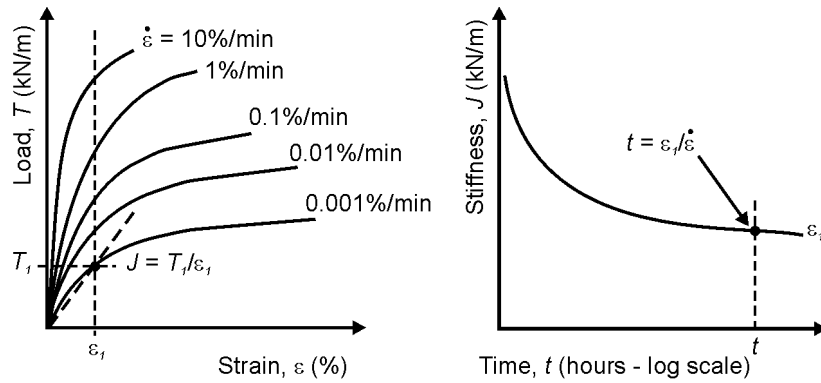
5. Based on the data available, the COV for extensometer readings was shown to be in the range of 29 to 56% for strains from 0.2 to 1%, but improved to a value of 9% if the devices are restricted to strains  $\geq 2\%$ .

Strategies to improve confidence with interpretation of strain readings from field monitoring are: use both strain gauges and extensometers; include multiple strain gauges at nominal identical locations in the wall, and; use strain gauge pairs mounted top and bottom at each reinforcement monitoring point (Gnanendran and Selvadurai 2001).

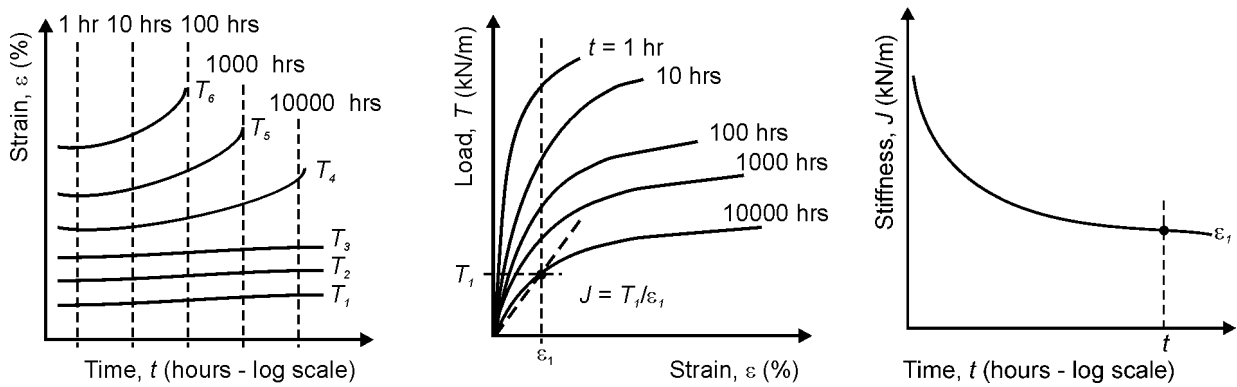
#### 4.2 Conversion of Geosynthetic Strain to Load using Reinforcement Stiffness

The second step in the calculation of reinforcement load from global strain is the selection of a suitable reinforcement stiffness value. The following variables will influence the magnitude of geosynthetic reinforcement stiffness in-situ at the end of construction (Bush 1990; Rimoldi and Montanelli 1993; Allen and Bathurst 1994; Boyle et al. 1996; Yuan et al. 1998):

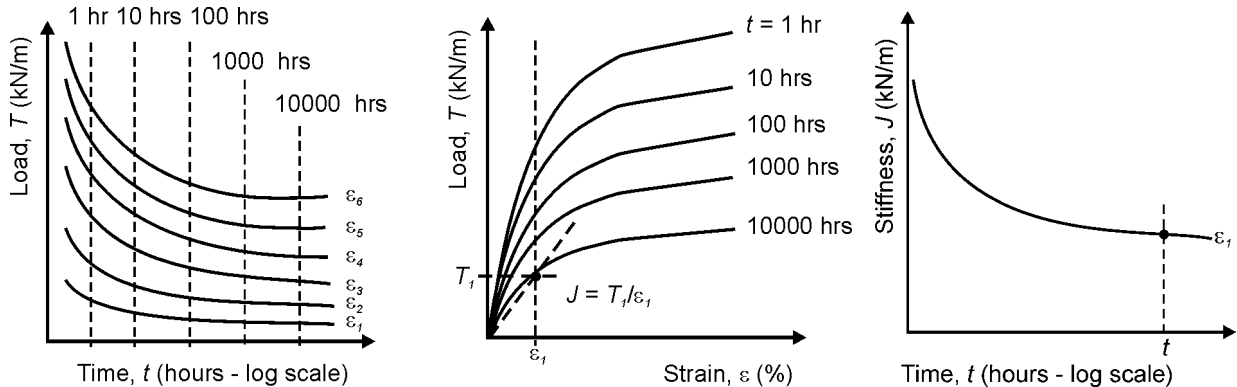
1. Loading sequence.
2. Rate of loading and time after application of load.
3. Soil confinement.
4. Strain level.
5. Temperature.
6. Installation damage



a) constant-rate-of-strain tests



b) constant load (creep) tests



c) constant strain (stress relaxation tests)

Figure 4. Determination of reinforcement stiffness values as a function of time using different laboratory test methods.

#### 4.2.1 Laboratory Test Methods

The stiffness of a geosynthetic at a given time or loading rate, strain level, and temperature is essentially the slope of a load-strain curve from a constant-rate-of-strain (CRS) tensile test, or the slope of an isochronous load-strain

curve from either a creep test or stress relaxation test. A secant slope is used to define the reinforcement stiffness in this paper. The stiffness obtained from a family of creep curves is denoted as the “creep stiffness” ( $J_c$ ) and similarly, the “relaxation stiffness” ( $J_r$ ) is obtained from a family of stress relaxation curves. The creep stiffness  $J_c$  (typically kN/m) is expressed as follows:

$$J_c = \frac{T_i}{\varepsilon_i} \quad [2]$$

where  $T_i$  is the load per metre width (kN/m) and  $\varepsilon_i$  is the strain at any time. The same equation can be used for the relaxation stiffness, although the magnitude of creep stiffness is not necessarily equal to the relaxation stiffness value.

Figure 4 illustrates the approach to determine the stiffness of a geosynthetic reinforcement product from each test method. The most common method to convert strain to load has been the in-isolation isochronous creep approach.

Walters et al. 2002 pointed out that the loading rate in a typical index test (ASTM D 4595) is approximately five orders of magnitude larger than the loading rate of the reinforcement in several example full-scale walls. This difference in loading rate leads to a large difference in the estimated stiffness value for the reinforcement at end-of-construction and beyond. For example, the simple use of stiffness values taken at 2% strain during an index CRS test run at 10% strain/minute (ASTM D 4595) can lead to an over-estimation of reinforcement loads for polyolefin products by a factor of 3 to 4 and, hence, lead to excessively conservative design. The corresponding error for PET products is less, resulting in an over-estimation of reinforcement loads in the range of about 20 to 30%.

In this study, 2% strain has been taken as a target value for selection of reinforcement stiffness values from in-isolation creep testing. With few exceptions, the corrected strain values in full-scale walls under working stress conditions were less than 2% (Bathurst et al. 2002). In addition, a 2% strain level facilitates estimation of reinforcement stiffness values from in-isolation laboratory test results. Finally, the use of a 2% stiffness value results in a conservative (i.e., safe) estimate of reinforcement load capacity for design.

Based on a review of published data for in-isolation creep and stress relaxation testing, Walters et al. (2002) observed the following general trends for stiffness values calculated at 2% strain:

1. Stiffness values decrease at a decreasing rate with logarithm of time for all the materials tested regardless of the method of test.
2. The stiffness of PET products is least affected by time compared to PP and HDPE geosynthetics, at least for strains up to 2%.
3. The relaxation stiffness value is typically less than the creep stiffness value for all three polymer types.
4. The stiffness values obtained from the different test methods tend to converge at longer times for PP geosynthetics (see example data in Figure 5). However, there was not a consistent trend regarding convergence or non-convergence for the PET and HDPE geosynthetic materials tested.

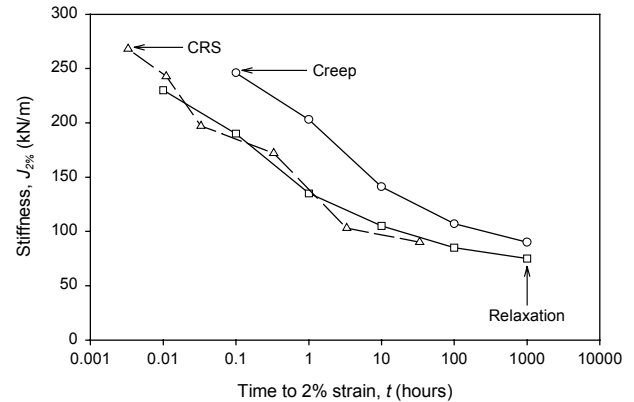


Figure 5. In-isolation CRS, creep and relaxation stiffness values at 2% strain for a biaxial PP geogrid (Walters et al. 2002).

5. The stiffness values obtained from the CRS tests as a function of time for HDPE and PP geosynthetics are roughly the same or slightly lower than the stiffness values obtained from creep testing, especially at longer times.
6. The stiffness curves based on creep testing are significantly flatter at elapsed times in excess of 100 hours which is less than the time required to construct walls in the field.

#### 4.3 Temperature and Installation Damage Effects

Temperature will affect the stiffness value of geosynthetics, with increasing temperature resulting in lower stiffness, especially for polyolefin materials (e.g., Bush 1990). Time-temperature superposition techniques are used to estimate the stiffness at any specific temperature (e.g., WSDOT 1998). The stiffness value used to estimate load from strain measurements should be determined at the temperature in the wall. Current US design practice considers the effective wall temperature to be the temperature that is the mean of the average yearly air temperature and the normal daily air temperature for the hottest month at the site (AASHTO 2002).

Allen and Bathurst (1994) investigated the effect of installation damage on the stiffness of different types of geosynthetic reinforcement. They determined that for woven geotextiles, the decrease in stiffness is minor for levels of damage that result in less than 40% peak tensile strength loss. For geogrids, the stiffness loss is insignificant until very high levels of damage are achieved.

Allen and Bathurst (1996) also investigated the combined effect of installation damage and creep on the strain response to load of various geosynthetics. They determined that the creep strain response is the same before and after installation damage, which indicates that the creep stiffness will also be the same before and after damage.

Table 1 provides data presented by Allen and Bathurst (1994) who quantified variability in stiffness values caused by installation damage. This table also shows the magnitude of COV values for different geosynthetics. From their test data, the writers concluded that the COV of the reinforcement stiffness at 2% strain, considering the effects of significant installation damage and time, can be expected to vary from 5 to 18% for geogrids to approximately 26% for woven geotextiles. If installation damage is light (say, strength losses less than 20%), the maximum COV values reported here will likely be less.

#### 4.4 Comparison of In-isolation and In-soil Test Results

The writers reviewed the effect of in-isolation and in-soil testing on the calculation of in-soil stiffness at the times of interest (100 to 1,000 hours or more) and found them to be relatively small. An example of stiffness values as a function of time for a woven geotextile tested under in-isolation and in-soil conditions is illustrated in Figure 6. For woven geotextiles and geogrids, soil confinement appears to have little effect on the stiffness (less than a 5 to 15% increase). Therefore, in-isolation testing should be sufficient for these materials. The available data show that the in-isolation creep tests gave the highest estimates of the long-term stiffness values. Thus the results of this test are conservative for the estimation of reinforcement loads in design. Furthermore, based on in-situ measured reinforcement strains in full-scale walls (Allen and Bathurst 2002), it appears that at the end of wall construction, the reinforcement tends to exhibit primarily creep, while at long times after construction, the reinforcement tends toward pure relaxation once the soil ceases to deform. Therefore, it can be concluded that the in-isolation creep test can be used to conservatively estimate the reinforcement stiffness at longer times (e.g., 500 to 1,000 hours or more) for woven geotextiles and geogrids for the purpose of calculating reinforcement loads in field-scale walls.

Table 1. Coefficient of variation (COV) of reinforcement CRS stiffness value ( $J_{crs}$ ) at 5% strain for geosynthetics in both virgin and damaged conditions (Walters et al. 2002).

| Product Type | Condition | COV (%) of CRS Stiffness Value at 5% Strain | % Increase in COV due to Damage |
|--------------|-----------|---|---------------------------------|
| Geotextile   | Virgin    | 10.3  | -                               |
|              | Damaged   | 15.2  | 47.6                            |
| HDPE Geogrid | Virgin    | 2.6   | -                               |
|              | Damaged   | 3.1   | 19.2                            |
| PET Geogrid  | Virgin    | 6.4   | -                               |
|              | Damaged   | 7.1   | 10.9                            |
| PP Geogrid   | Virgin    | 8.2   | -                               |
|              | Damaged   | 10.3  | 25.6                            |

Note: All tests carried out at 10% strain/minute.

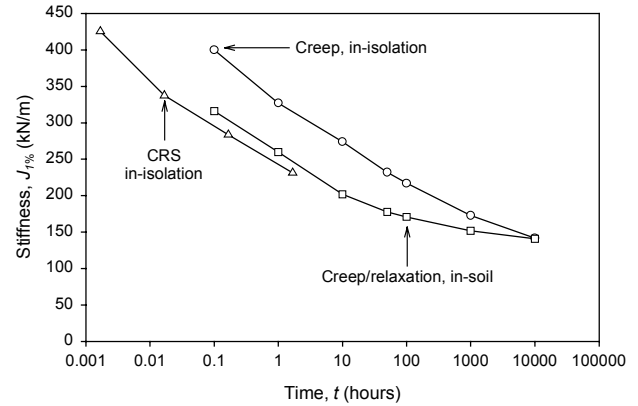


Figure 6. Comparison of CRS and isochronous creep stiffness values at 1% strain from in-isolation and in-soil tests on woven PP geotextile (data from Boyle 1995).

#### 4.5 Approach to Determine Reinforcement Stiffness Values

For geogrids and woven geotextiles (the most common reinforcement products for reinforced soil walls) the writers have developed the following procedure to estimate the in-soil stiffness value:

1. Determine the total length of time it will take to complete construction of the reinforced soil structure at a given section (i.e., the time after which no additional loading will occur – limited data available to the writers shows that field walls are typically constructed in 500 to 1500 hours).
2. Using the procedures illustrated in Figure 4, develop an in-isolation creep stiffness versus time curve at constant strain levels of interest, and select the creep stiffness based on the elapsed time to the end of wall construction. Select the stiffness at the anticipated maximum working strains for the wall, as the stiffness is likely to be strain level dependent. For design purposes, a 2% secant stiffness at 1,000 hours is reasonable. If strains of 3 to 4% or more are anticipated, determine the stiffness at the higher strain level. If strains significantly less than 2% are anticipated, and a geosynthetic material is being used which is known to have a highly non-linear load-strain curve over the strain range of interest (e.g., some PET geosynthetics), then a stiffness value determined at a lower strain should be considered.
3. If the effective site temperature is anticipated to be significantly different from 20°C, the creep stiffness value may need to be temperature shifted, requiring creep data at higher or lower temperatures to establish the appropriate shift factors. See Bush (1990) for an example of temperature shifting.

Correct the stiffness obtained in step 3 for soil confinement effects if the reinforcement is not a geogrid or slit film woven geotextile. For multi-filament woven geotextiles, the in-isolation stiffness may need to be

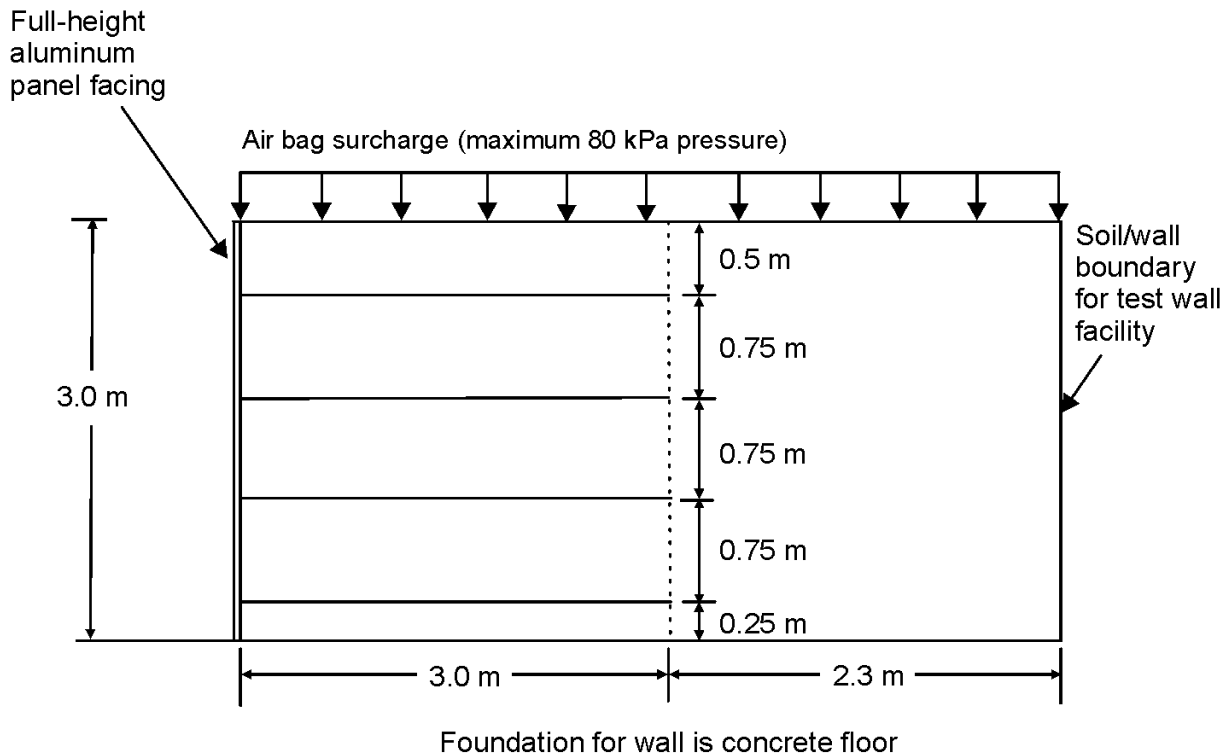


Figure 7. Cross-section of RMC full-height propped aluminum panel wall constructed with PP geogrid reinforcement layers (Wall GW14 – Bathurst and Benjamin 1990).

increased by a factor of 1.1 to 1.2 and for nonwoven geotextiles by a factor of 2 to 5.

Estimates of the ratio of creep stiffness value at typical working conditions (i.e., strains at (say) 2% and loading times of 1000 hours) to the stiffness value from a conventional CRS test (ASTM D 4595) are summarised in Table 2. This table is useful for estimating reinforcement stiffness values in the absence of in-solation laboratory test data.

Table 2. Ratio of typical working stress stiffness (at 1,000 hours) to the stiffness obtained in a CRS test at 10%/minute, per ASTM D 4595 (Walters et al. 2002).

| Geosynthetic Polymer | $J_{1000 \text{ hours}}/J_{D 4595}$ |
|----------------------|-------------------------------------|
| PP                   | 0.25 to 0.35                        |
| HDPE                 | 0.25 to 0.35                        |
| PET                  | 0.75 to 0.85                        |

#### 4.6 Accuracy of Stiffness Value and Estimate of Error in Calculation of Reinforcement Load

The calculation of reinforcement load  $T$  based on best estimates of stiffness and strain values is made using the following expression:

$$T_i = J_c \times \varepsilon_i \quad [3]$$

Associated with each load value is uncertainty in the predicted value that varies with the magnitude of the estimate of error of the stiffness and strain measurements as noted earlier. Uncertainty in strain measurements ( $COV_\varepsilon$ ) and stiffness values ( $COV_J$ ) are uncorrelated (i.e. independent). Therefore, total uncertainty in estimated reinforcement loads can be quantified by a coefficient of variation ( $COV_T$ ) value calculated as follows (Ang and Tang 1975):

$$COV_T = \sqrt{COV_\varepsilon^2 + COV_J^2} \quad [4]$$

This approach is used to calculate the error bars in the plots for estimated reinforcement load values presented later in the paper.

#### 4.7 Example Wall GW14

Figure 7 shows a propped panel faced geogrid wall was built to full scale in the laboratory to a maximum height of 3.0 m (Bathurst and Benjamin 1990). Figure 8 shows measured and predicted connection loads for this wall. Reinforcement loads were measured directly by load cells at the connection with the facing and estimated from strains measured using strain gauges and extensometers attached to the reinforcement just beyond the load cells. Error bars in the figure represent  $\pm 1$  standard deviation

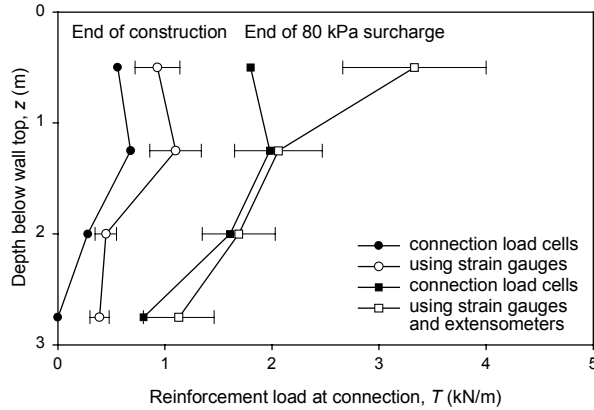


Figure 8. Measured reinforcement connection loads and connection loads predicted from strain gauge and extensometer measurements (Wall GW14 – Walters et al. 2002).

on estimates of reinforcement load using strain gauge and extensometer readings. The load levels at the connection from the load cells are slightly lower than those estimated from the strain gauge readings. The high load estimated using the strain gauge in the top reinforcement layer relative to the load measured by the load cell may be attributed to the vertical settlement of the soil directly behind the facing, leading to the generation of additional down-drag strains. The strain gauges are able to record additional strains due to changes in reinforcement out-of-plane geometry while the load cells were configured to record only the in-plane horizontal load in the reinforcement. Notwithstanding the complications noted above, the measured loads and estimated loads from interpretation of reinforcement strains are considered to be in reasonable agreement.

## 5. COMPARISON OF MEASURED LOADS WITH CURRENT PRACTICE

The methodologies described in the preceding sections can now be used to estimate reinforcement loads in the full-scale reinforced soil walls investigated by the writers (Section 2) and these loads used to examine the accuracy of predicted loads using current North American practice.

### 5.1 Simplified Method

The primary design method in North America for geosynthetic reinforced soil walls is called the Tieback Wedge or Simplified Method (AASHTO 1996, 2002). In this approach the wall is assumed for internal design to be flexible with enough deformation to generate an active state of stress. Hence, the lateral earth pressure coefficient  $K_a$  is used to convert vertical stress to lateral stress.  $K_a$  is determined in this method assuming a horizontal backslope and no wall-soil interface friction in all cases. The reinforcement is assumed to resist lateral stresses occurring within the wall, with each reinforcement layer designed to resist the lateral stress

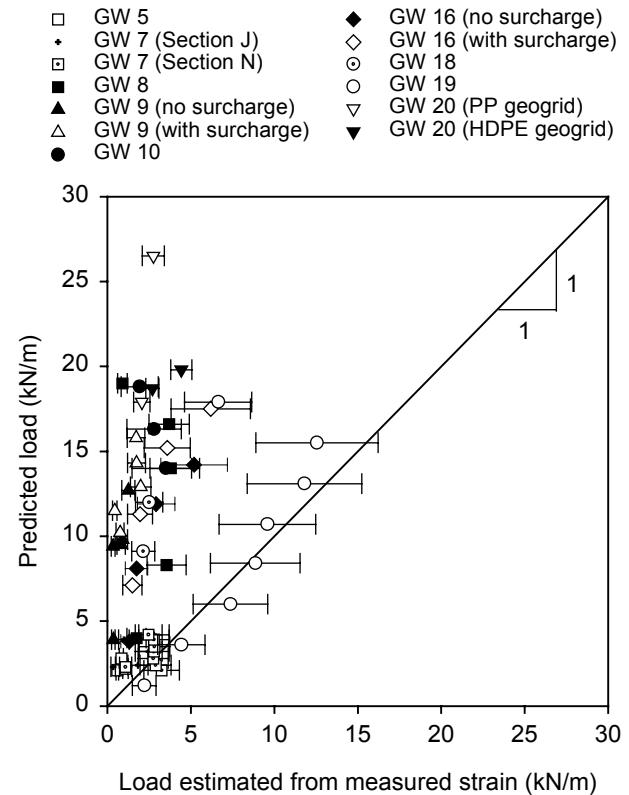


Figure 9. Predicted versus reinforcement load estimated from strain measurements for full-scale field geosynthetic walls, using the AASHTO Simplified Method and triaxial or direct shear peak shear strength values (Allen and Bathurst 2002).

over a tributary area. The Rankine failure wedge is held in horizontal equilibrium by the reinforcement layers that act as tiebacks. The maximum tensile load in a reinforcement layer,  $T_{max}$  (in units of force per running unit length of wall) is calculated according to:

$$T_{max} = S_v K_a (\gamma [z + S] + q) \quad [5]$$

where,  $S_v$  = tributary area (assumed equivalent to the vertical spacing of the reinforcement when analyses are carried out per unit length of wall),  $K_a$  = active lateral earth pressure coefficient,  $\gamma$  = soil unit weight,  $z$  = depth to the reinforcement level relative to the wall top at the wall face,  $S$  = average soil surcharge depth above the wall top, and  $q$  = vertical stress due to traffic surcharge.

### 5.2 Comparison of Predicted and Estimated Loads

Figure 9 illustrates how well the Simplified Method predicts reinforcement loads in geosynthetic walls built in the field. The error bars in the figure show the variance ( $\pm 1$  standard deviation) in the “best estimate of measured” reinforcement loads based on the estimate of uncertainty in strain and reinforcement stiffness measurements. Note that triaxial or direct shear peak soil friction angles

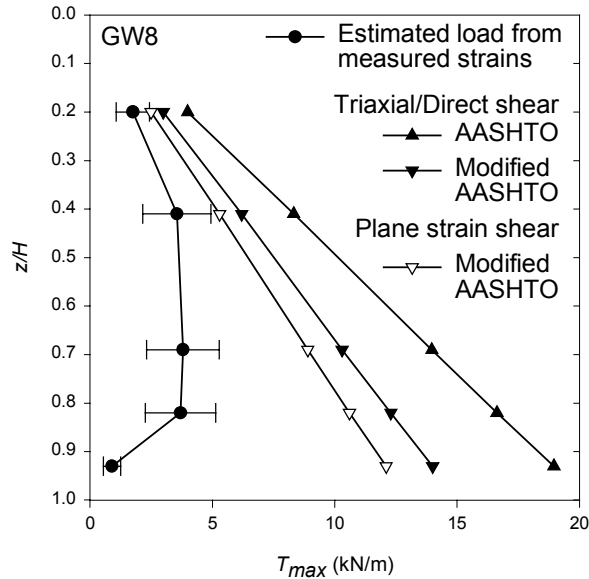


Figure 10. Predicted peak reinforcement loads, and peak loads estimated from measured strains (Wall GW8 – Allen et al. 2002). Note: Error bars represent best estimate of measured load  $\pm 1$  standard deviation.

and unit weights estimated from measured data were used to calculate loads. Plane strain conditions likely prevail in these types of reinforced structures (Rowe and Ho 1993; Zornberg et al. 1998) but it is recognised that in practice triaxial or direct shear backfill friction angles would be used with this design method (AASHTO 2002). No safety factors were applied to calculate the predicted loads.

The data in Figure 9 show that there is a tremendous amount of scatter in the predicted loads. Furthermore, with the exception of two walls (GW 19 and GW 7) the general trend is that the predicted loads are greater than the estimated loads. Interestingly, Walls GW 19 and GW 7 are a sloped-face wall ( $27^\circ$  facing batter) and a polymer strip reinforced soil wall, respectively, and are excluded as geosynthetic reinforced soil walls in current practice (Elias et al. 2001; AASHTO 2002).

Allen and Bathurst (2002) also compared the distribution of estimated reinforcement load and predicted loads under working load levels for the case study walls in this investigation. An example comparison is shown in Figure 10. The modified AASHTO curves refer to the use of the horizontal component of earth pressure in Equation 5 which reduces the magnitude of earth force calculated for each reinforcement layer. The data in the figure show that reinforcement loads were excessively conservative for this structure and that the trend towards increasing reinforcement load with depth below the top of the wall was not captured using the Simplified Method. The magnitudes of predicted load were also reduced by using plane strain friction angle values for the soil backfill. This result suggests that a significant source of conservatism

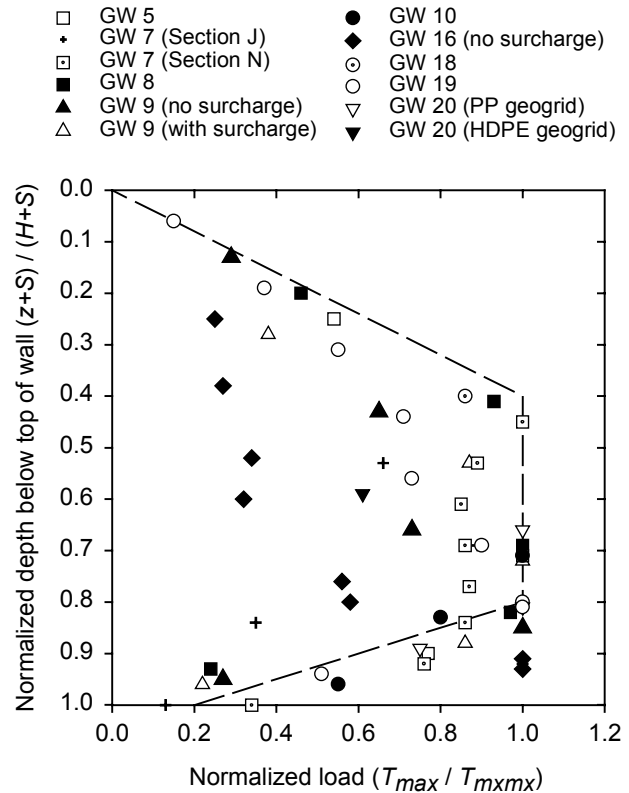


Figure 11. Normalized reinforcement loads estimated from strain measurements as a function of normalized depth below wall top (Allen et al. 2003).

in current design practice is the use of laboratory shear strength values that are not corrected for the plane strain conditions that prevail in most geosynthetic reinforced soil wall structures.

Figure 11 shows the distribution of reinforcement loads ( $T_{max}$ ) estimated from measured strains in the full-scale field walls, normalised to the maximum reinforcement load within the wall ( $T_{maxmx}$ ). The normalised loads are plotted against the relative depth below the elevation of the average soil surcharge height to account for the effect of surcharge on reinforcement load near the top of the wall. The load distribution envelope is not triangular as is currently assumed for design, but rather is trapezoidal in shape. An approximate trend line is superimposed on the data in the figure to help emphasise the shape of the load distribution envelope in the figure.

The explanation for the reduction in reinforcement loads at the base of the walls in Figures 10 and 11 is proximity to the stiff foundation base and toe restraint at the wall footing. Analysis of a series of RMC walls has shown that the combination of the wall face and wall toe restraint carries a significant portion of the internal load for geosynthetic walls, thereby reducing the load the reinforcement must carry. The stiffer the wall face/wall toe restraint, the less load the reinforcement must carry (Bathurst et al. 2000, 2001). The contribution of facing stiffness and toe restraint is not explicitly considered in

the AASHTO Simplified Method and is an important source of conservatism in current design practice.

### 5.3 Soil Failure as a Limit State in Wall Design

Included in the database of walls was one full-scale wrapped-face field wall (Allen et al. 1992) and a series of full-scale laboratory walls constructed at RMC (Bathurst et al. 2000, 2001) that were taken to load levels in excess of “working load” levels. This state was achieved through the application of a uniform surcharge pressure applied at the surface of the wall backfill starting at the crest of the wall. Bathurst and co-workers noted that in their full-scale laboratory tests, soil failure occurred before reinforcement rupture. Evidence of soil failure, defined as the internal development of a contiguous soil failure zone in the reinforced soil mass, included a sudden and large outward movement of the wall face, soil settlement directly behind the wall face and a concurrent increase in reinforcement strains. In some cases, further increases in surcharge loading lead to reinforcement rupture and collapse of the wall.

The performance of these walls prior to collapse was used to delineate walls that can be expected to have good long-term performance (see Section 3) from walls with poor performance. Direct measurement of soil shear strains consistent with the notion of soil plasticity (failure) was not possible. However, as a general rule, reinforcement strains in excess of 3% strain were shown to be a quantitative indicator of soil failure. Reinforcement strains in excess of this value are believed to lead to soil softening and the shedding of soil load capacity to the reinforcement layers. From a practical point of view, restricting reinforcement strains from achieving tensile strains in excess of 3% strain can be used to prevent soil failure and represents an important limit state that should be considered in the development of working stress wall design methodologies.

## 6. A NEW WORKING STRESS METHOD FOR PREDICTION OF REINFORCEMENT LOADS IN GEOSYNTHETIC WALLS

The previous section has highlighted deficiencies in the current Simplified Method with respect to the calculation of reinforcement loads for internal stability design of geosynthetic reinforced soil walls. A subset of the database of case studies collected by the writers (16 fully instrumented walls and 14 walls with limited measurements) was used to develop a new design methodology based on working stress principles. “Best estimate” reinforcement loads under working load levels were used to calibrate this empirical-based design method. The methodology is called the “K-Stiffness Method” (Allen et al. 2003; Allen and Bathurst 2003) and is briefly described in the following sections.

### 6.1 Background

The following key factors will influence the magnitude of maximum reinforcement load,  $T_{max}$ :

1. Height of the wall and any surcharge loads.
2. Global and local stiffness of the soil reinforcement.
3. Resistance to lateral movement caused by the stiffness of the facing and restraint at the wall toe.
4. Face batter.
5. Shear strength and stress-strain behaviour (e.g., modulus) of the soil.
6. Unit weight of the soil.
7. Vertical spacing of the reinforcement.

It is useful to note at this point that items 2, 3 and 4 are not considered in the Simplified Method. Of particular importance is the possible effect of magnitude of reinforcement stiffness on the magnitude and distribution of reinforcement loads as demonstrated in physical tests and numerical models (Christopher 1993; Bathurst and Hatami 1998).

In the K-Stiffness Method, the contribution of these key factors to the calculation of the maximum load in a reinforcement layer  $i$  is expressed as:

$$T_{max}^i = \frac{1}{2} K \gamma (H + S) S_V^i D_{tmax} \Phi_g \Phi_{local} \Phi_{fs} \Phi_{fb} \quad [6]$$

where:  $K$  = lateral earth pressure coefficient;  $\gamma$  = unit weight of the soil;  $H$  = height of the wall;  $S$  = equivalent height of uniform surcharge pressure  $q$  (i.e.,  $S = q/\gamma$ );  $S_V^i$  = tributary area (equivalent to the vertical spacing of the reinforcement in the vicinity of each layer when analyses are carried out per unit length of wall);  $D_{tmax}$  = load distribution factor that modifies the reinforcement load based on layer location. The remaining terms,  $\Phi_g$ ,  $\Phi_{local}$ ,  $\Phi_{fs}$  and  $\Phi_{fb}$  are influence factors that account for the effects of global and local reinforcement stiffness, facing stiffness and face batter, respectively. The coefficient of lateral earth pressure  $K$  is calculated using the Jaky equation (Holtz and Kovacs 1981) together with  $\phi_{ps}$  = peak plane strain friction angle of the soil. The use of  $K = K_o$  in this proposed method does not imply that at-rest conditions exist within the reinforced backfill.  $K_o$  is simply used as a familiar index parameter to characterise soil behaviour.

The empirical reinforcement load distribution parameter  $D_{tmax}$  is used to distribute the load as a function of depth, accounting for the reinforcement properties, load redistribution among layers, and foundation conditions. It is expressed here as a function of normalized depth below the top of the wall  $(z+S)/(H+S)$ , including the effect of the soil surcharge  $S$ , and varies over the range  $0 \leq D_{tmax} \leq 1$ . The distribution is illustrated by the dashed lines in Figure 11.

Parameter  $\Phi_g$  is a global stiffness factor that accounts for the influence of the stiffness and spacing of the reinforcement layers over the entire wall height and has the general form:

$$\Phi_g = \alpha \left( \frac{S_{\text{global}}}{p_a} \right)^\beta \quad [7]$$

Here,  $S_{\text{global}}$  is the global reinforcement stiffness and  $\alpha$  and  $\beta$  are constant coefficients. The non-dimensionality of the expression is preserved by dividing the global reinforcement stiffness by  $p_a = 101$  kPa (atmospheric pressure). The global reinforcement stiffness value for a wall is calculated as (Christopher et al. 1990):

$$S_{\text{global}} = \frac{J_{\text{ave}}}{(H/n)} = \frac{\sum_{i=1}^n J_i}{H} \quad [8]$$

Here,  $J_{\text{ave}}$  is the average tensile stiffness of all “n” reinforcement layers over the wall height and,  $J_i$  is the tensile stiffness of an individual reinforcement layer expressed in units of force per unit length of wall.

Parameter  $\Phi_{\text{local}}$  is a local stiffness factor that accounts for the relative stiffness of the reinforcement layer with respect to the average stiffness of all reinforcement layers and is expressed as:

$$\Phi_{\text{local}} = \left( \frac{S_{\text{local}}}{S_{\text{global}}} \right)^a \quad [9]$$

$S_{\text{local}}$  is the local reinforcement stiffness for reinforcement layer  $i$  calculated as:

$$S_{\text{local}} = \left( \frac{J}{S_v} \right)_i \quad [10]$$

Local deviations from overall trends in reinforcement loads can be expected when the reinforcement stiffness and/or spacing of the reinforcement change from average values over the height of the wall (i.e.,  $S_{\text{local}}/S_{\text{global}} \neq 1$ ; Hatami et al. 2001). This effect is captured by the local stiffness factor  $\Phi_{\text{local}}$  expressed by Equation 9.

Parameters  $\Phi_{\text{fs}}$  (facing stiffness factor) and  $\Phi_{\text{fb}}$  (facing batter factor) in Equation 6 are factors that account for the influence of the facing stiffness and facing batter, respectively, and are constant values for a given wall.

## 6.2 Results of Back-analyses

The values for the influence factors introduced above are assumed to be uncorrelated to facilitate back-analysis. Individual values were back-calculated by rewriting Equation 6 to isolate each factor and using baseline values for the remaining influence factors and best

estimates of reinforcement loads and stiffness values. For example, the results of regression analysis gave values of  $\alpha = 0.25$  and  $\beta = 0.25$  for the power function described by Equation 7.

Regression analyses using Equation 9 gave  $a = 1$  for geosynthetic reinforced soil walls. To accommodate a seamless transition to steel reinforced soil walls, a similar back-analysis by Allen and Bathurst (2003) gave  $a = 0$  for steel soil reinforcement systems.

For preliminary design purposes, the following facing stiffness factor values are recommended:

1.  $\Phi_{\text{fs}} = 0.35$  for modular block and propped concrete panel faced walls (stiff facings).
2.  $\Phi_{\text{fs}} = 0.5$  for incremental precast concrete facings.
3.  $\Phi_{\text{fs}} = 1.0$  for all other types of wall facings (flexible facings - e.g., wrapped-face, welded wire or gabion faced).

The influence of wall facing batter on maximum reinforcement loads is adjusted in the proposed working stress method using an empirical facing batter factor expressed as:

$$\Phi_{\text{fb}} = \left( \frac{K_{\text{abh}}}{K_{\text{avh}}} \right)^d \quad [11]$$

where:  $K_{\text{abh}}$  = horizontal component of active earth pressure coefficient accounting for wall face batter;  $K_{\text{avh}}$  = horizontal component of active earth pressure coefficient (assuming the wall is vertical) and;  $d$  = constant coefficient. The form of the equation shows that as the wall face batter angle  $\omega \rightarrow 0$  (i.e., wall facing batter approaches the vertical) the facing batter factor  $\Phi_{\text{fb}} \rightarrow 1$ . A value of  $d = 0.25$  gives the best fit based on the available  $T_{\text{max}}$  data and is recommended as the default value in the proposed K-Stiffness Method.

## 6.3 Overall Performance of the K-Stiffness Method

The accuracy of the proposed K-Stiffness Method (Equation 6) for geosynthetic walls is illustrated in Figure 12. The improvement over the Simplified Method is apparent when this figure is compared to Figure 9. Similarly, the improved performance of the K-Stiffness Method over the Simplified Method with respect to the distribution of loads in reinforced soil walls is apparent in Figure 13. The relative improvement of the K-Stiffness Method over the Simplified Method can also be quantified by examining the ratio of the measured to predicted reinforcement loads (bias) and the spread in the bias values (Table 3). A bias value of one is desirable. The lower the COV of the bias values the better the accuracy of the model. In both cases the K-Stiffness Method is superior to the Simplified Method.

The strain level in the reinforcement also appears to have a significant effect on the prediction accuracy of the K-Stiffness Method. Figure 14 shows predicted

reinforcement strains using the K-Stiffness Method and  $T_{\text{max}}$ , plotted against the measured reinforcement strains for geosynthetic walls. The predicted strains were calculated by dividing  $T_{\text{max}}$  by the reinforcement layer secant modulus,  $J$  (see Equation 3). It appears that once reinforcement strains exceed approximately 3 to 4% for the available case histories, the K-Stiffness Method consistently under-predicts the measured strain. It should be noted that all of the strains greater than about 3% were measured in full-scale test walls which were surcharged to loads well in excess of working stress conditions (see Bathurst 1993; Bathurst et al. 1993, 2000, 2001 for details regarding these full-scale test walls).

Table 3. Ratio of Measured to Predicted Reinforcement Loads (Bias) (Allen et al. 2003).

|                         | Simplified Method | K-Stiffness Method |
|-------------------------|-------------------|--------------------|
| Mean $T_{\text{max}}$   | 0.65              | 0.99               |
| COV $T_{\text{max}}$    | 95%               | 36%                |
| Mean $T_{\text{maxmx}}$ | 0.58              | 0.99               |
| COV $T_{\text{maxmx}}$  | 99%               | 17%                |

$T_{\text{max}}$  = maximum load in a reinforcement layer

$T_{\text{maxmx}}$  = maximum load in wall from all layers

COV = standard deviation of bias/mean of bias x 100%

It should also be noted in Figure 14 that at high reinforcement strains the walls with stiff facings plot consistently below the walls with flexible facings. This may be an indicator that the facing stiffness correction factor used in the K-Stiffness method is not a constant as proposed, but increases toward 1.0 (i.e., less effect of facing stiffness) as strain increases. At higher strains, the facing appears to have reduced reserve capacity to carry additional load (Bathurst et al. 2000). While the facing has not failed at reinforcement strains greater than 1.5 to 2%, the reinforcement takes on additional load to maintain facing column equilibrium. Once reinforcement strains exceed 3 to 4%, the soil begins to fail for both flexible and stiff-faced walls.

Geosynthetic reinforcement can reach much higher strains without failure than the soil. Therefore, prevention of reinforcement failure, an objective of current internal stability design methods, does not ensure against failure of a geosynthetic wall due to failure of the backfill soil. Prevention of reinforcement strains (over the design life of the structure) that are great enough to allow failure of the soil should be an objective of any working stress design method. Soil failure is defined as contiguous or near-contiguous zones of soil with shear strains in excess of the strain at peak strength. Contiguous shear zones have been observed in test walls taken to collapse under uniform surcharge loading (Bathurst 1990, Bathurst et al. 1993). Once the soil has failed, for all practical purposes the wall has failed and an internal strength limit state achieved.

- GW5
- + GW7, Section J
- ⊙ GW7, Section N
- GW8
- ▲ GW9, no surcharge
- △ GW9, with surcharge
- GW10, with water restraint removed
- ◆ GW16, no surcharge
- ◇ GW16, with surcharge
- ⊙ GW18
- GW19
- ▼ GW20, HDPE Section
- ▽ GW20, PP Section

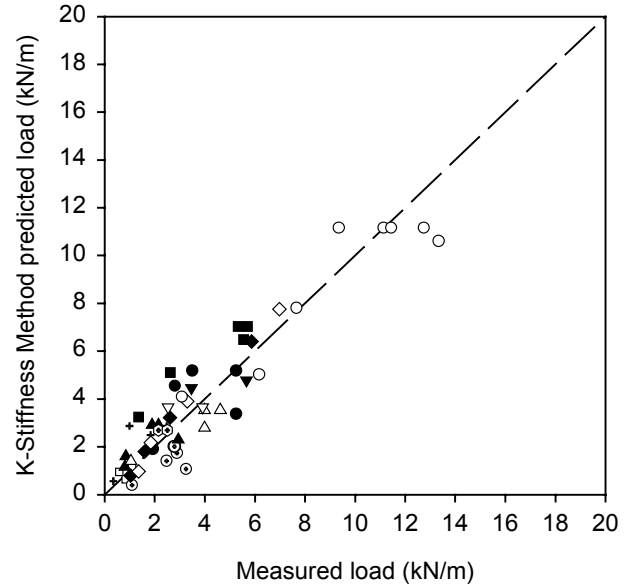
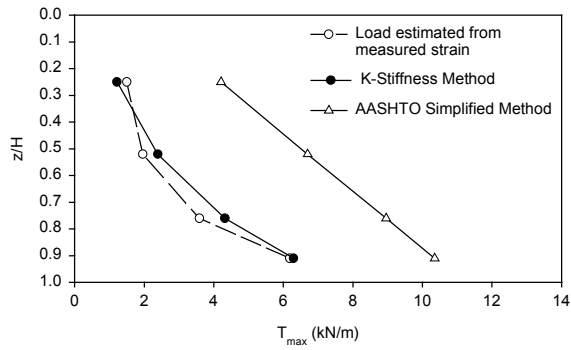


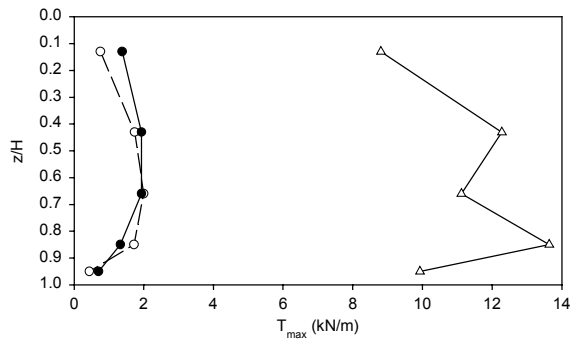
Figure 12. Predicted versus measured values of  $T_{\text{max}}$  in reinforcement layers for geosynthetic walls, using the K-Stiffness Method (Allen and Bathurst 2003).

Plane strain shear strength data for the backfill used in one case study wall (GW16) indicated that the soil had peak strains on the range of 2 to 3% (Boyle 1995). Since the backfill used for this wall was at the upper end regarding shear strength for the case histories considered herein, these plane strain peak strains are likely at the lower end of the typical range for granular soils. Plane strain shear strength data reported by Lee (2000) for RMC soil specimens at confining pressures comparable to surcharge pressures required to initiate large wall deformations indicate that peak soil strains in the walls were about 2 to 3%. In both cases (Boyle 1995; Lee 2000), the plane strain test results indicated that the peak soil strain increases with increasing confining stress.

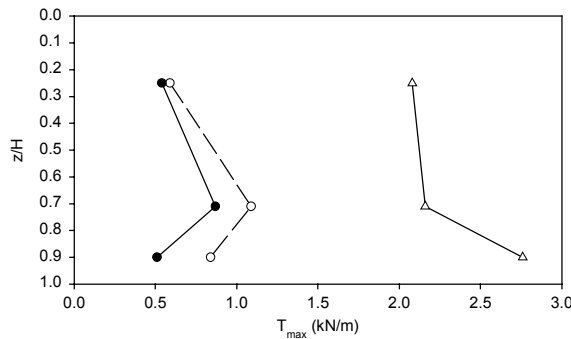
Based on data from the RMC full-scale walls, geosynthetic reinforcement tensile strains large enough to cause signs of soil failure are typically numerically greater than the 2 to 3% peak soil shear strain values required to generate a contiguous failure zone in these walls, as shown in Figure 14. Furthermore, Figure 14 shows that for the available data, the K-Stiffness Method provides an accurate prediction of reinforcement strains up to reinforcement strain levels that are numerically at or slightly greater than the soil peak shear strain (i.e., reinforcement strain levels of approximately 3% or more that appear to correspond to soil peak shear strains of 2 to 3% based on laboratory plane strain testing of granular soils used in full-scale walls). A direct theoretical



a) GW16 (wrapped-face wall) with soil surcharge



b) GW9 (modular block wall) with soil surcharge



c) GW5 (incremental precast concrete panel wall)

Figure 13. Predicted load and distribution versus measured values of  $T_{max}$  in reinforcement layers for geosynthetic walls, using the K-Stiffness Method (Allen and Bathurst 2003).

relationship between reinforcement tensile strain, soil shear strain, and the onset of soil failure is difficult to accomplish at present. However, based on the empirical evidence available, it appears that preventing the reinforcement strain from exceeding a 3% design value will be adequate for the high shear strength granular backfill soils in this study and likely a lower bound (conservative) estimate for design using weaker backfill

soils. Nevertheless, the relationship between reinforcement strain and the soil shear strain at peak strength needs to be investigated for a wider range of soils.

## 7. CONCLUSIONS

This paper traces a body of work by the writers that has identified significant deficiencies in the current AASHTO Simplified Method for the design of reinforcement layers against over-stressing in internal stability calculations. Excessive conservatism using the AASHTO method has been demonstrated to lead to reinforcement volumes that may be twice that required to achieve the good wall performance observed in a database of walls that have performed well for up to 18 years. These structures can be reasonably expected to continue to perform well through the remainder of their design life (e.g., reinforcement strain rates and wall deformations have stopped).

A database of wall case studies comprised of structures with a typical range of geometry and geosynthetic reinforcement products has been used to calculate actual reinforcement loads. These values have been used to calibrate a new working stress method which provides a framework to capture the influence of reinforcement stiffness, layer arrangement, facing type, soil properties and duration of loading on the magnitude and distribution of reinforcement loads. A novel feature of this new method is to design the wall reinforcement so that the soil within the wall backfill is prevented from reaching a state of failure, consistent with the notion of working stress conditions. This concept represents a new approach for internal stability design of geosynthetic reinforced soil walls because prevention of soil failure as a limit state is considered in addition to the current practice of preventing reinforcement rupture.

## ACKNOWLEDGEMENTS

The writers would like to acknowledge the opportunity afforded by the International Society of Soil Mechanics and Geotechnical Engineering, the International Geosynthetics Society and Tensar International to present this synthesis of work as the Mercer Lecture for 2002-2004. The writers would also like to acknowledge the financial support of the following State Departments of Transportation: Washington, Alaska, Arizona, California, Colorado, Idaho, Minnesota, New York, North Dakota, Oregon, Utah, and Wyoming. The writers are also grateful for the financial support from the Natural Sciences and Engineering Research Council of Canada, Academic Research Program of the Department of National Defence (Canada) and grants from the Department of National Defence, Canada. Finally, the writers are indebted to R.R. Berg, W.F. Lee, and R.D. Holtz through collaboration on some of the papers cited herein, and B.B. Christopher and J.R. Bell for many fruitful discussions over many years.

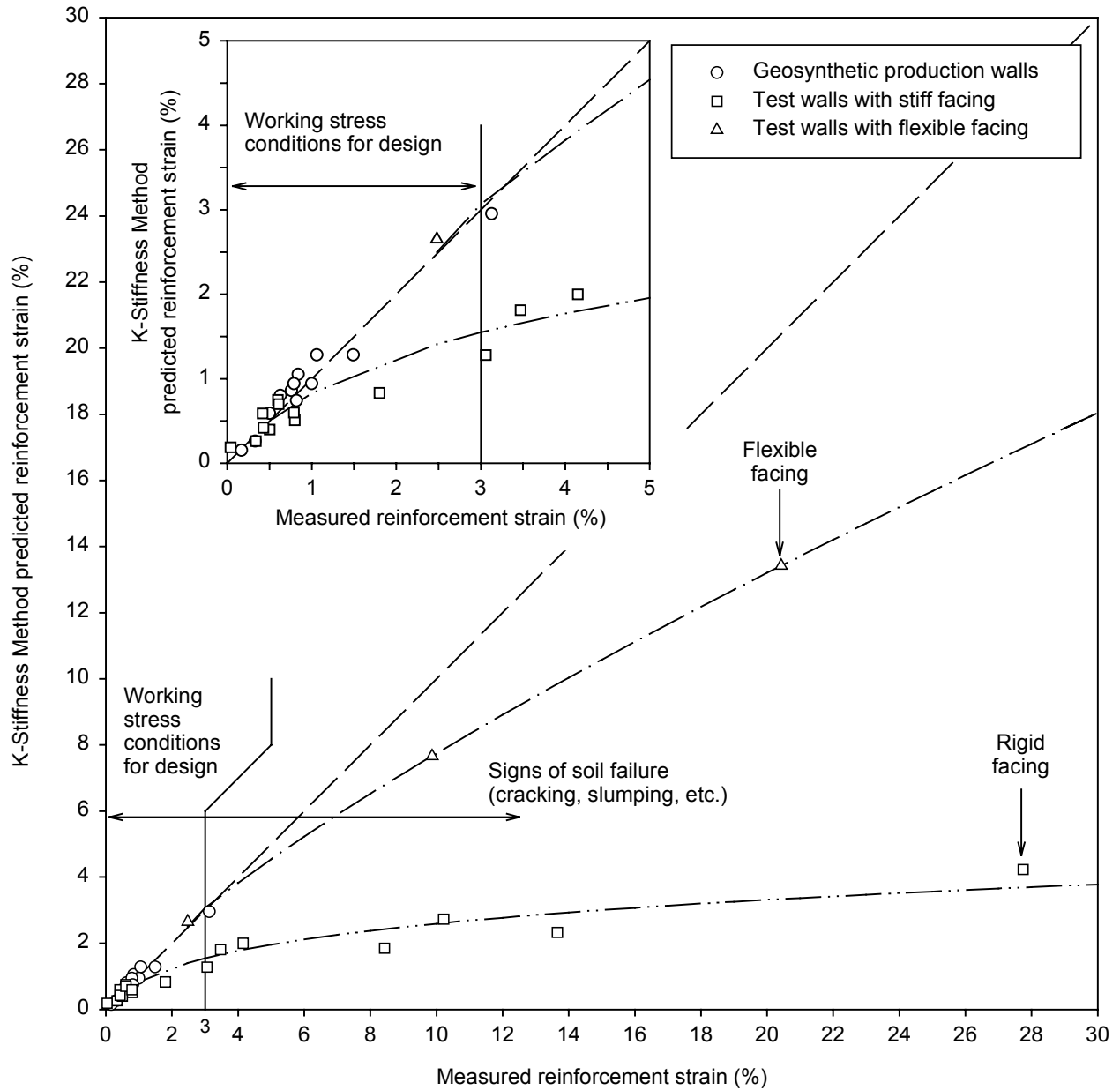


Figure 14. Predicted versus measured reinforcement strain (based on  $T_{max}$ ) using the K-Stiffness Method for full-scale production (field) and full-scale laboratory geosynthetic walls, a) inset showing 0 to 5% reinforcement strain range (Allen et al. 2003).

## REFERENCES

- AASHTO. 1996. Standard Specifications for Highway Bridges. American Association of State Highway and Transportation Officials, Sixteenth Edition, Washington, D.C.
- AASHTO. 2002. Standard Specifications for Highway Bridges. American Association of State Highway and Transportation Officials, Seventeenth Edition, Washington, D.C.
- Allen, T.M., and Bathurst, R.J. 1994. Characterization of Geosynthetic Load-Strain Behavior After Installation Damage. *Geosynthetics International*, 1 (2): 181-199.
- Allen, T.M., and Bathurst, R.J. 1996. Combined Allowable Strength Reduction Factor for Geosynthetic Creep and Installation Damage. *Geosynthetics International*, 3 (3): 407-439.
- Allen, T.M., and Bathurst, R.J. 2002. Observed Long-Term Performance of Geosynthetic Walls, and Implications for Design. *Geosynthetics International*, 9 (5-6): 567-606.
- Allen, T.M., and Bathurst, R.J. 2003. Prediction of Reinforcement Loads in Reinforced Soil Walls. Washington State Department of Transportation, Report WA-RD 522.2.
- Allen, T.M., Bathurst, R.J., and Berg, R.R. 2002. Global Level of Safety and Performance of Geosynthetic Walls: An Historical Perspective. *Geosynthetics International*, 9 (5-6): 395-450.
- Allen, T.M., Christopher, B.R., and Holtz, R.D. 1992. Performance of a 12.6 m High Geotextile Wall in Seattle, Washington. In Proceedings of the International Symposium on Geosynthetic-Reinforced Soil Retaining Walls, Denver, Colorado. Edited by J.T.H. Wu. Balkema, Rotterdam, pp. 81-100.
- Allen, T.M., Bathurst, R.J., Lee, W.F., Holtz, R.D., and Walters, D.L. 2003. A New Working Stress Method for Prediction of Reinforcement Loads in Geosynthetic Walls. (in press) *Canadian Geotechnical Journal*.
- Ang, A.H-S., and Tang, W.H. 1975. Probability Concepts in Engineering Planning and Design: Volume 1 – Basic Principles. John Wiley and Sons, New York, NY, USA.
- ASTM D 4595. Standard Test Method for Tensile Properties of Geotextiles by the Wide-width Strip Method. In 1996 Annual Book of ASTM Standards. ASTM, West Conshohocken, Pennsylvania.
- Bathurst, R.J. 1990. Instrumentation of Geogrid-Reinforced Soil Walls. Transportation Research Record No. 1277, Washington, DC, pp. 102-111.
- Bathurst, R.J. 1992. Case Study of a Monitored Propped Panel Wall. In Proceedings of the International Symposium on Geosynthetic-Reinforced Soil Retaining Walls, Denver, Colorado. Edited by J.T.H. Wu. Balkema, Rotterdam, pp. 159-166.
- Bathurst, R.J. 1993. Investigation of Footing Restraint on Stability of Large-Scale Reinforced Soil Wall Tests. In Proceedings of the 46th Annual Canadian Geotechnical Conference, Saskatoon, Saskatchewan, pp. 389-398.
- Bathurst, R.J., and Benjamin, D.J. 1990. Failure of a Geogrid-Reinforced Soil Wall. Transportation Research Board 1288, pp. 109-116.
- Bathurst, R.J., and Hatami, K. 1998. Seismic Response Analysis of a Geosynthetic Reinforced Soil Retaining Wall. *Geosynthetics International*, 5 (1-2): 127-166.
- Bathurst, R.J., Allen, T.M., and Walters, D.L. 2002. Short-Term Strain and Deformation Behavior of Geosynthetic Walls at Working Stress Conditions. *Geosynthetics International*, 9 (5-6): 451-482.
- Bathurst, R.J., Jarrett, P.M., and Benjamin, D.J. 1993. A Database of Results from an Incrementally Constructed Geogrid-Reinforced Soil Wall Test. *Reinforcement Des Sols: Experimentations en Vraie Grandeur des Annees 80*, Paris, pp. 401-430.
- Bathurst, R.J., Walters, D.L., Hatami, K., and Allen, T.M. 2001. Full-scale Performance Testing and Numerical Modelling of Reinforced Soil Retaining Walls. Special Invited Lecture. In International Symposium on Earth Reinforcement, IS Kyushu 2001, Fukuoka, Japan, Vol. 2, pp. 777-799.
- Bathurst, R.J., Walters, D., Vlachopoulos, N., Burgess, P., and Allen, T.M. 2000. Full Scale Testing of Geosynthetic Reinforced Walls. Invited keynote paper. In Proceedings of Geo-Denver 2000. American Society of Civil Engineers. Edited by J.G. Zornberg and B.R. Christopher. ASCE Special Publication No. 103, Advances in Transportation and Geoenvironmental Systems using Geosynthetics, pp. 201-217.
- Bolton, M.D. 1986. The strength and dilatancy of sands. *Geotechnique*, 36 (1): 65-78.
- Boyle, S.R. 1995. Deformation Prediction of Geosynthetic Reinforced Soil Retaining Walls. Ph.D. thesis, University of Washington, Washington.
- Boyle, S.R., Gallager, M. and Holtz, R.D. 1996. Influence of Strain Rate, Specimen, Length and Confinement on Measured Geotextile Properties. *Geosynthetics International*, 3 (2): 205-225.
- Bush, D.I. 1990. Variation of Long-Term Design Strength of Geosynthetics in Temperatures up to 40°C. In Proceedings of the Fourth International Conference on Geotextiles, Geomembranes, and Related Products, The Hague, Netherlands, pp. 673-676.
- Christopher, B.R. 1993. Deformation Response and Wall Stiffness in Relation to Reinforced Soil Wall Design. Ph.D. Thesis, Purdue University, Indiana.
- Christopher, B.R., Gill, S.A., Giroud, J.-P., Juran, I., Mitchell, J.K., Schlosser, F., and Dunncliff, J. 1990. Reinforced Soil Structures Vol. 1: Design and Construction Guidelines. FHWA Report FHWA-RD-89-043.
- Elias, V., Christopher, B.R., and Berg, R.R. 2001. Mechanically Stabilized Earth Walls and Reinforced Soil Slopes - Design and Construction Guidelines. FHWA-NHI-00-043, Federal Highway Administration, Washington, DC.

- Fannin, R.J. 1988. Soil Reinforcement for Norwegian Conditions - An Instrumented Field Study of the Analysis and Design of Geogrid Reinforced Slopes. Norwegian Geotechnical Institute, Report 52757-10.
- Fannin, R.J., and Hermann, S. 1990. Performance Data for a Sloped Reinforced Soil Wall. Canadian Geotechnical Journal, 27: 676-686.
- Gnanendran, C.T., and Selvadurai, A.P.S. 2001. Strain Measurement and Interpretation of Stabilizing Force in Geogrid Reinforcement. Geotextiles and Geomembranes, 19: 177-194.
- Hatami, K., Bathurst, R.J., and Di Pietro, P. 2001. Static Response of Reinforced Soil Retaining Walls with Non-Uniform Reinforcement. International Journal of Geomechanics, 1 (4): 477-506.
- Holtz, R.D., and Kovacs, W. D. 1981. An Introduction to Geotechnical Engineering. Prentice-Hall, Inc., New Jersey.
- Jewell, R.A., and Wroth, C.P. 1987. Direct Shear Tests on Reinforced Sand. Geotechnique, 37 (1): 53-68.
- Lade, P.V., and Lee, K.L. 1976. Engineering Properties of Soils. Report UCLA-ENG-7652. University of California, Los Angeles.
- Lee, W.F. 2000. Internal Stability Analysis of Geosynthetic Reinforced Retaining Walls. Ph.D. Thesis, University of Washington, Washington.
- Perkins, S.W., and Lapeyre, J.A. 1997. In-Isolation Strain Measurement of Geosynthetics in Wide-Width Strip Tension Test. Geosynthetics International, 4 (1): 11-32.
- Rimoldi, P., and Montanelli, F. 1993. Creep and Accelerated Creep Testing for Geogrids. In Proceedings of Geosynthetics '93, Vancouver, British Columbia, Canada, April 1993, Vol. 2, pp. 773-787.
- Rowe, R.K., and Ho, S.K. 1993. Keynote Lecture: A Review of the Behavior of Reinforced Soil Walls. In Proceedings of the International Symposium on Earth Reinforcement Practice, Vol. 2. Edited by H.Ochiai, S. Hayashi, and J. Otani, Balkema, pp. 801-830.
- Walters, D., Allen, T.M., and Bathurst, R.J. 2002. Conversion of Geosynthetic Strain to Load using Reinforcement Stiffness. Geosynthetics International, 9 (5-6): 483-523.
- WSDOT. 1998. Determination of Long-term Strength of Geosynthetics. WSDOT Test Method 925, Washington State Department of Transportation, FOSSC Materials Laboratory, Tumwater, WA, USA.
- Yuan, Z., Swan, R.H., Jr., and Bachus, R.C. 1998. Soil Confinement Effect on Stress-Strain Properties of Geosynthetics. In Proceedings of the Sixth International Conference on Geosynthetics, Vol. 2, Atlanta, GA, March 1998, pp. 523-528.
- Zornberg, J.G., Sitar, N., and Mitchell, J.K. 1998. Limit Equilibrium as Basis for Design of Geosynthetic Reinforced Slopes. Journal of Geotechnical and Geoenvironmental Engineering, 124 (8): 684-698.